Peridotite xenoliths from the Morrón de Villamayor volcano (Calatrava Volcanic Field)

Xenolitos peridotíticos del volcán Morrón de Villamayor (Campo Volcánico de Calatrava)

Javier García Serrano[1], Carlos Villaseca[2] and Cecilia Pérez-Soba[2]

[1] Dpto. Mineralogía y Petrología. Facultad CC. Geológicas. Universidad Complutense de Madrid.
[2] Instituto de Geociencias IGEO (UCM, CSIC).

ABSTRACT

*The El Morrón de Villamayor (MVM) peridote xenoliths vary from orthopyroxene-poor lherzolite to wehrlite in modal composition. This compositional feature contrasts with other Calatrava (CVF) xenolith suites. The studied xenoliths equilibrated at lower temperatures (618-942 °C) and slightly shallower (8.8-13.6 kbar) conditions than other CVF peridotites. MVM peridotites show local intense interaction with the host leucitite displaying spongy rims around primary clinopyroxene and also reaction zones with K-rich minerals (*e.g.*, sanidine, leucite and richterite) and widespread clinopyroxene, olivine and spinel neoblasts. Nevertheless, the orthopyroxene-poor character of MVM peridotites might be caused by some previous metasomatic event.*

Key-words: *peridotite xenoliths, leucitite melt, wehrlite, Calatrava Volcanic Field.*

RESUMEN

Los xenolitos peridotíticos del volcán El Morrón de Villamayor (MVM) son lherzolitas pobres en ortopiroxeno y wehrlitas, en contraste con los datos previos de xenolitos de otros volcanes de Calatrava. Las peridotitas estudiadas están equilibradas a temperaturas más bajas (618-942 °C) y menor profundidad (8,8-13,6 kbar) que las estimadas en otras peridotitas del Campo Volcánico de Calatrava. Localmente hay una intensa interacción del fundido leucitítico con los minerales primarios de la peridotita, ya que se originan zonas de reacción con minerales ricos en K (p.ej., sanidina, leucita y richterita) y frecuentes neoblastos de clinopiroxeno, olivino y espinela. El carácter pobre en ortopiroxeno de las peridotitas MVM debe estar causado por algún evento metasomático previo.

Palabras clave: *xenolitos peridotíticos, fundido leucitítico, wehrlita, Campo Volcánico de Calatrava.*

Geogaceta, 67 (2020), 43-46
ISSN (versión impresa): 0213-683X
ISSN (Internet): 2173-6545

Fecha de recepción: 24/06/2019
Fecha de revisión: 17/10/2019
Fecha de aceptación: 22/11/2019

Introduction

Ultramafic xenoliths carried by alkaline volcanic magmas provide crucial information about the subcontinental lithospheric mantle. In this work, we characterize the mantle of central Spain by studying peridotite xenoliths from the El Morrón de Villamayor volcanic center (MVM), which belongs to the Calatrava Volcanic Field (CVF).

The CVF is a Neogene anorogenic intracontinental zone within the circum-Mediterranean province (Lustrino and Wilson, 2007). This volcanic field includes more than 200 volcanic vents in an area of around 5500 km^2 (Ancochea, 1982; Cebriá, 1992).

The Calatrava volcanism occurred during two different stages (Ancochea, 1982). The first stage was a minor ultrapotassic event around 8.7-6.4 my ago, which originated the studied MVM volcanic center. A second widespread stage (3.7 to 0.7 Ma) generated volcanic centers of sodic alkaline magmatism, some of them carrying mantle xenoliths that have been previously studied: El Palo (Bianchini *et al*., 2010), Cerro Pelado (Villaseca *et al*., 2010), El Aprisco (Villaseca *et al*., 2010, González-Jiménez *et al*., 2014; Lierenfeld and Mattsson, 2015; Puelles *et al*., 2016; Villaseca *et al*., 2019) and Los Tormos (Andía *et al*., 2018) volcanoes.

Petrographic characterization of host magma and mantle xenoliths

The MVM is a small (<1 km^2) monogenetic volcanic edifice with an outstanding chemical and isotopic composition compared to the rest of studied volcanic centers of the CVF (*e.g.*, López-Ruiz *et al*., 1993; Lustrino *et al*., 2019). The volcanic peak poured out a set of highly porphyritic olivine leucitite lava flows showing large (up to 7 mm) olivine macrocrysts.

Within these lava flows, centimeter-sized mantle xenoliths appear. We have selected for this work a dozen of representative peridotite xenoliths with different compositional and textural features. The sampled mantle xenoliths are thin slices of small size (<7 cm in maximum length) showing evidence of interaction with the host melt. These mantle xenoliths display a coarse- to medium-grained protogranular texture, except three samples that present fine-grained equigranular texture. One xenolith shows traces of mineral orientation.

Modal analyses were performed, but due to the small size of the xenoliths the results may be considered as rough estimations. Peridotites are mostly classified as lherzolites, and three samples plot in the wehrlite field. This compositional range is markedly lower in orthopyroxene modal amount than other suites of the CVF (Fig. 1A).

The peridotites consist of olivine, clinopyroxene, orthopyroxene, spinel and reaction zones rich in secondary minerals. One lherzolite sample (116442) has a minor amount of spinel. No hydrous metasomatic minerals have been found in the MVM mantle xenoliths.

There are evidences that host leucitite melt affected these mantle xenoli-

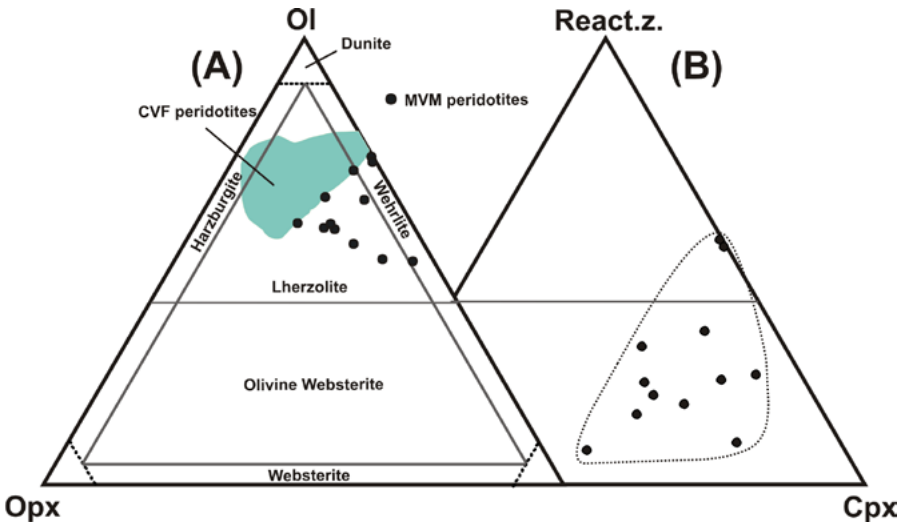

Fig. 1.– A) Modal classification of the MVM xenoliths using the IUGS scheme (Le Maitre *et al.*, 2002). B) Modal composition including the amount of reaction zones (React.z.) of the MVM xenoliths. See color figure in the web.
Fig. 1.– A) Análisis modales de los xenolitos del MVM. B) Composición modal incluyendo la proporción de las zonas de reacción (React.z.) Ver figura en color en la web.

ths. Thus, an increase of spongy texture in clinopyroxene crystal rims appears, mostly in those close to the xenolith margin (Fig. 2). This secondary clinopyroxene hosts glass microinclusions and vugs similar to those described by Pan *et al*. (2018). Moreover, complex reaction zones are also common towards the contact with the host leucitite (up to 21 vol.%, Fig. 1B). In these areas, primary peridotite minerals have been transformed to secondary neoblasts of spinel, clinopyroxene and olivine, together with interstitial richterite amphibole, sanidine, leucite, K-rich nepheline, sulfur drops within interstitial glass, and local carbonate patches.

Reaction zones show locally some textural zoning. Thus, sieved textures appear on crystal rims of primary peridotite minerals (zone 1), evolving towards granoblastic aggregates of micro-neoblasts (zone 2), and further on micro-symplectitic intergrowths of ol-2 and cpx-2 towards the center of these areas (zone 3). The mineral chemistry of spongy types when compared to neoblasts is slightly different as shown below.

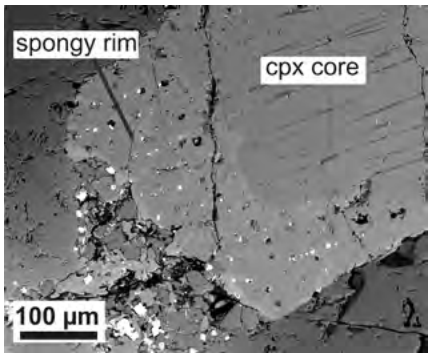

Fig. 2. - Spongy clinopyroxene towards the contact with host leucitite.
Fig. 2. - Clinopiroxeno criboso próximo al contacto con la leucitita olivínica.

Mineral Chemistry

Olivine

The Mg number [#Mg = 100*Mg / (Mg + Fe^{2+}) on molar basis] of primary olivine mostly ranges from 89.7 to 90.9, except for sample 116442, which has lower olivine modal amount, showing a higher #Mg (91.4-91.9) than other MVM mantle xenoliths. Secondary olivine display higher MgO and CaO contents, as observed in other xenolith suites (Villaseca et al., 2010; Andía et al., 2018).

Orthopyroxene

#Mg varies from 89.6 to 91.5, but again lherzolite 116442 shows higher #Mg (91.8–92.7) values. Orthopyroxene from this sample shows the lowest Al_2O_3 and the highest Cr_2O_3 contents of the MVM peridotite xenolith suite.

Clinopyroxene

Similary to olivine and orthopyroxene, sample 116442 has clinopyroxene with higher #Mg (92.9–93.9) than other MVM mantle xenoliths (90.4–92.7). It also displays lower Al_2O_3, Na_2O and TiO_2 (Fig. 3B) but higher Cr_2O_3 contents (Fig. 3A).

Spongy clinopyroxene shows higher CaO and TiO_2, and lower Na_2O and Al_2O_3 contents than primary clinopyroxene, and plots in different compositional fields with respect to the small cpx-2 neoblasts of reaction zones 2 and 3 (Fig. 3).

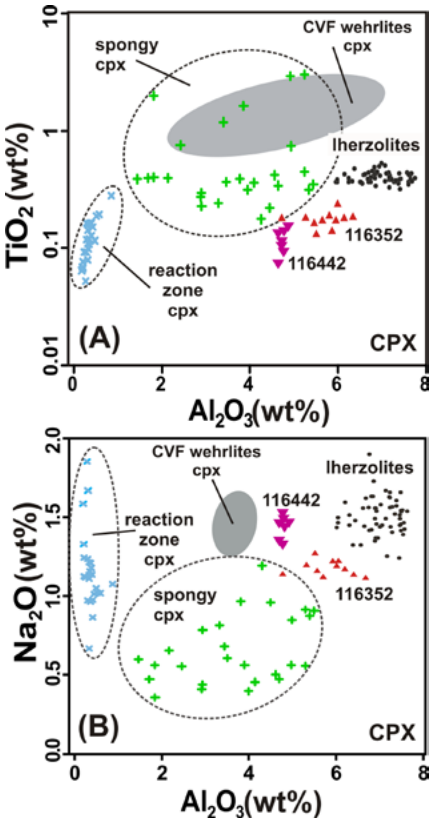

Fig. 3.– A) Al_2O_3 vs. TiO_2, and B) Al_2O_3 *vs.* Na_2O diagrams of clinopyroxene, compared to other CVF wehrlites from Andía *et al.* (2018) and Villaseca *et al.* (2010). See color figure in the web.
Fig. 3.– Diagramas (A) Al_2O_3 **vs.** *TiO_2, y (B) Al_2O_3* **vs.** *Na_2O de clinopiroxenos, comparados con los de wehrlitas de otros centros volcánicos del Campo Volcánico de Calatrava (Andía* **et al.**, *2018; Villaseca* **et al.**, *2010). Ver figura en color en la web.*

Spinel

Two types of spinel can be distinguished. Primary spinel is characterized by low Cr_2O_3 (8.7–12.7 wt%) and high Al_2O_3 (49.7–52.6 wt%) contents, as in other Calatrava xenolith suites. However, spinel in lherzolite 116352 shows slightly higher Cr_2O_3 (16.5–17.9 wt%) and lower Al_2O_3 (49.7–52.6 wt%) contents (Fig. 4).

Secondary spinel from reaction zones displays higher and wider Cr_2O_3 (12.0–20.0 wt%) and lower Al_2O_3 (45.8–53.9 wt%) contents than primary spinel, being remarkable its high TiO_2 (0.35–3.0 wt%, Fig. 4) and FeO (13–28.7 wt%) contents.

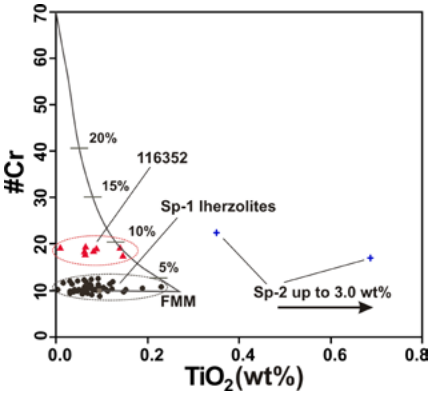

Fig. 4.– TiO_2 *vs.* Cr number [#Cr = 100*Cr / (Cr + Al) on molecular basis] diagram of spinel. The trend of partial melting of a fertile MORB mantle (FMM) is shown for comparison. See color figure in the web.
Fig. 4.– Diagrama TiO_2 **vs.** *número de Cr [#Cr = 100*Cr / (Cr + Al) en valores moleculares] en espinela. Se muestra para comparar la pauta de fusión de un manto tipo MORB (FMM). Ver figura en color en la web.*

Geothermobarometry

The lack of garnet in the mantle xenoliths of the MVM volcano constrains pressure estimation depth to less than 60 km (pressure <17 kbar). We have used geobarometer estimates by Nimis and Ulmer (1998) on clinopyroxene composition. Estimated pressure in the MVM xenoliths ranges from 8.8 to 13.6 kbar. The lowest pressure estimate corresponds to the orthopyroxene-poor lherzolite 116442.

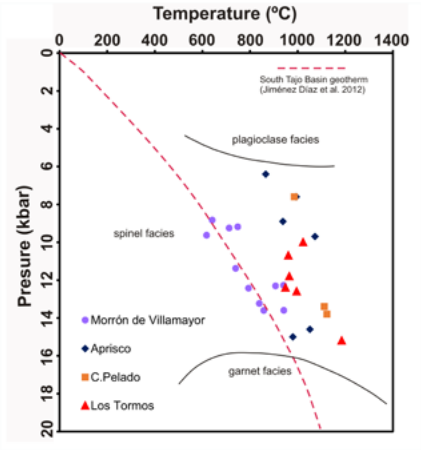

Fig. 5.– Pressure *vs.* temperature diagram estimated by using the geobarometer of Nimis and Ulmer (1998) and the two-pyroxene geothermometer of Brey and Köhler (1990), compared with results from the Aprisco and the Cerro Pelado xenolith estimates (Villaseca *et al.*, 2010). See color figure in the web.
Fig. 5– Diagrama de presión **vs.** *temperatura estimados usando el geobarómetro de Nimis y Ulmer (1998) y el geotermómetro de dos piroxenos de Brey y Köhler (1990). Se compara con los xenolitos del Aprisco y el Cerro Pelado (Villaseca* et al.*, 2010). Ver figura en color en la web.*

Temperatures calculated on the basis of the two pyroxene geothermometer of Brey and Kohler (1990) range from 618 to 942 ºC (at pressures previously estimated). These temperatures are notably lower than other estimates in CVF peridotite xenolith suites (Bianchini *et al.*, 2010; Villaseca et al., 2010; Andía *et al.*, 2018) (Fig. 5). Importantly, the MVM peridotite temperatures are mostly aligned with the south Tajo basin geotherm estimated by Jiménez-Díaz *et al.* (2012). The lower temperature of the MVM xenoliths could be due to the eccentric position of the MVM volcano respect to the main CVF, with a higher volcanic center concentration, suggestive of a major thermal input in this mantle sector.

Discussion

Orthopyroxene-poor xenolith suite

The MVM peridotite modal composition is based only on preserved primary minerals (79 to 97 vol.% of rock), which define the orthopyroxene-poor character of this suite. The limited amount of reaction zones indicates that leucitite melt infiltration cannot change significantly the orthopyroxene-poor character of the MVM xenoliths.

Therefore, MVM xenoliths might have undergone a previous alkaline silica-undersaturated metasomatic event inducing the orthopyroxene-poor singularity of these peridotites. At least, three alkaline metasomatic events of different ages (Cretaceous, Eocene and Miocene) have been described in the CVF (Villaseca *et al.*, 2019). Correlation with any of those old magmatic events requires further study on mineral trace element contents of cryptically metasomatized minerals.

The chemical composition of the MVM wehrlite clinopyroxene does not overlap the fields of other studied CVF wehrlite xenoliths (Villaseca *et al.*, 2010; Andía *et al.*, 2018), indicating that MVM Opx-poor xenoliths are not the consequence of reaction with Fe-Ti-rich silica-undersaturated melts of the Calatrava volcanism, as was suggested in those studies on the origin of the Cerro Pelado or Los Tormos wehrlites.

Partial melting of the mantle sources

According to the #Cr *vs.* TiO_2 diagram for spinel in MVM peridotite xenoliths (Fig. 4), most xenoliths display low partial melting degrees (5%), except for lherzolite 116352 (7-10%). This moderate degree of partial melting is in the range obtained in other CVF peridotite suites (Villaseca *et al.*, 2010; Andía *et al.*, 2018).

Decompression during transport

The high Al^{IV}/Al^{VI} ratios shown by spongy clinopyroxene is a decompression indicator (Aoki and Kushiro, 1968; Su *et al.*, 2011). The MVM spongy and reactional clinopyroxene neoblasts have higher Al^{IV}/Al^{VI} ratios than primary clinopyroxene (Fig. 6), suggesting an origin by decompression during host-melt reaction. Pressure estimates on secondary clinopyroxene yield markedly lower values (1.3–-4.5 kbar) than on primary clinopyroxene.

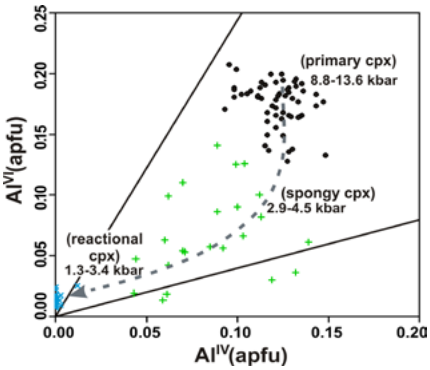

Fig. 6.– Al^{IV} *vs.* Al^{VI} diagram of MVM peridotite clinopyroxene defining a decompression trend from primary to secondary phases. See color figure in the web.
Fig. 6.– Diagrama de Al^{VI} **vs.** *Al^{IV} en clinopiroxenos de xenolitos del volcán MVM mostrando la tendencia de descompresión de tipos primarios a secundarios. Ver figura en color en la web.*

Conclusions

The composition of the lithospheric mantle sampled by the olivine leucitite magmas of the MVM volcano contrasts markedly in modal analyses with other CVF xenolith suites. Its composition varies from orthopyroxene-poor lherzolites to wehrlites. In the xenoliths studied, the leucitite host magma locally interacted with all the main peridotite minerals generating K-rich minerals within reaction zones (*e.g.*, sanidine, leucite, amphibole or K-rich nepheline). Nevertheless, the original modal compositions are not substantially modified out of these zones and preserve the original orthopyroxene-poor character of the MVM xenolith suite.

The chemical composition of the primary MVM clinopyroxene contrast with wehrlites of other xenolith suites from the CVF. Most of the CVF wehrlites might be originated by Fe-Ti metasomatism via sodium alkaline host melt-peridotite reaction, but the metasomatic agent that generated the MVM wehrlites and the orthopyroxene-poor signature of associated lherzolites is still not identified. Due to the early character of the ultrapotassic magmatism in the CVF, it is suggested that previous alkaline silica-undersaturated events have played a role in the origin of the Opx-poor signature of the MVM xenolith suite.

Finally, the mantle below the MVM volcano is markedly cold, probably due to its eccentric position with respect to the main effusive area of the CVF.

Acknowledgments

We thank Alfredo Fernández Larios for his assistance with the electron microprobe analyses in the Centro Nacional de Microscopía Electrónica (UCM). We acknowledge Manuel Díaz Azpiroz (editor), David Orejana and an anonymous reviewer their helpful comments on an earlier version of this paper. This work is included in the objectives and supported by the CGL2016-78796 project of the Spanish Ministerio de Ciencia e Innovación (MICINN), and the UCM 910492 group.

References

Ancochea, E. (1982). *Evolución espacial y temporal del volcanismo reciente de España Central*. Tesis Doctoral, UCM, Madrid, 675 p.

Andía, J., Villaseca, C. and Pérez-Soba, C. (2018). *Geogaceta* 63, 99-102.

Aoki, K.I. and Kushiro, I. (1968). *Contributions to Mineralogy and Petrology* 18, 326-337.

Bianchini, G., Beccaluva, L., Bonadiman, C., Nowell, G.M., Person, D.G., Siena, F. and Wilson, M. (2010). *Geological Society, London, Special Publications* 337, 107-124.

Brey, G.P. and Köhler, T. (1990). *Journal of Petrology* 31, 1353-1378.

Cebriá, J.M. (1992). *Geoquímica de las rocas basálticas de la región volcánica de Campo de Calatrava, España*. Tesis Doctoral, UCM, Madrid, 314 p.

González-Jiménez, J.M., Villaseca, C., Griffin, W.L., O'Reilly, S.Y., Belousova, E., Ancochea, E. and Pearson, N.J. (2014). *Contributions to Mineralogy and Petrology* 168, 1047, 24 p.

Jiménez-Díaz, A., Ruiz, J., Villaseca, C., Tejero, R. and Capote, R. (2012). *Journal of Geodynamics* 58, 29-37.

Le Maitre, R.W., Streckeisen, A., Zanettin, B., Le Bas, M.J., Bonin, B. and Bateman, P. (Eds.) (2005). *Igneous rocks: a classification and glossary of terms*. Cambridge University Press, Cambridge, 233 pp.

Lierenfeld, M.B. and Mattsson, H.B. (2015). *International Journal of Earth Sciences* 104, 1795-1817.

López-Ruiz, J., Cebriá, J.M., Doblas, M., Oyarzun, R., Hoyos, M. and Martín, C. (1993). *Journal of the Geological Society, London* 150, 915-922.

Lustrino, M. and Wilson, M. (2007). *Earth Science Reviews* 81, 1-65.

Lustrino, M., Fedele, L., Agostini, S., Prevelic. D., Salari, G. (2019). *Lithos* 324-325, 216-233.

Nimis, P. and Ulmer, P. (1998). *Contributions to Mineralogy and Petrology* 133, 122-135.

Pan, S., Zheng, J., Yin, Z., Griffin, W.L., Xia, M., Lin, A. and Zhan, H. (2018). *Journal of Petrology* 320-321, 144-154.

Puelles, P., Ábalos, B., Gil Ibarguchi, J.I., Carracedo, M. and Fernández-Armas, S. (2016). *Tectonophysics* 683, 200-215.

Su, B.X., Zhang, H.F., Sakyi, P.A., Yang, Y.H., Ting, J.F. and Ma, Y.G. (2011). *Contributions to Mineralogy and Petrology* 161, 465-482.

Villaseca, C., Ancochea, E., Orejana, D. and Jeffries, T.E. (2010). *Geological Society, London, Special Publications* 337, 125-151.

Villaseca, C., Belousova, E., Barfod, D., González-Jiménez, J.M. (2019). *Lithosphere* 11, 192-208.